Adsorption of the Phosphate Groups on Silica Hydroxyls: An ab Initio Study

Vladimir V. Murashov*

Department of Chemistry, University of British Columbia, Vancouver, British Columbia V6T 1Z1, Canada

Jerzy Leszczynski

Department of Chemistry, Jackson State University, Jackson, Mississippi 39217-0510

Received: April 24, 1998; In Final Form: November 19, 1998

Adsorption of the phosphate groups on a silica surface is investigated by ab initio calculations of hydrogen-bond complexes of dihydrogen and dimethyl phosphate anions with orthosilicic acid. It is found that the phosphate groups can form strong hydrogen-bonded complexes with the silanols of the silica surface with stabilization energies of ca. −14 kcal/mol per hydrogen bond. The effect of the coordination of the phosphate species by water, orthosilicic acid, and a sodium cation on the geometry and stability of the *-sc/-sc* conformation is investigated through consideration of 2-fold axial symmetry complexes. Calculations suggest the reduction of the COPO torsion angle of the *-sc/-sc* conformation of the phosphodiester backbones upon adsorption of molecules containing these moieties on silica compared to the value of this angle found for phosphates in vacuo and in hydrated forms. Both the polarizing and electron density abstracting abilities of silanols cause electron density redistribution, giving rise to strengthening of the phosphoester P−O bonding, weakening of the phosphinyl P═O and ester C−O bonding in adsorbed phosphate moieties. A very strong band at 3300 cm^{-1} appearing during the phosphate adsorption on the silanol hydroxyls is suggested for use as an indication of this phenomenon.

1. Introduction

Silicon dioxide, in pure form or in combination with other metal oxides (silicates), is the most abundant substance on earth, and for that reason it is destined to influence most processes taking place on our planet to some extent, including organic reactions occurring in living systems (some aluminosilicates are even considered by one of the popular hypotheses concerning the origins of life on earth as a substrate for and/or integral part of probiotic life forms[1]). Interaction of silica with organic matter is well-known: substituted silicates were found to form complexes with nucleosides through proton transfer,[2] to catalyze polymerization reactions, and to synthesize organic molecules from inorganic matter, thereby promoting the synthesis of amino acids as well as purines, pyrimidines, and carbohydrates. In addition, silicates were shown to catalyze the polymerization of amino acids into polypeptides.[3] Such activity of silica is believed to be connected with the available hydrogens and hydroxyls of the Si−OH surface groups and with the adsorption properties of silica surfaces and their polarization capabilities.

Silica particles entering living organisms become actively involved in biological processes. It seems that this compound exerts the most prominent effect on living cells in connection with its binding to the phosphate groups. Phosphate, a substituted derivative of orthophosphoric acid, H_3PO_4, and its deprotonated forms are some of the most important chemical entities present in living systems. Attention to the issue of phosphates binding to a silica surface has been intensified in connection with the discovered carcinogenic properties of a crystalline polymorph of silica, quartz, in vivo.[4] Another factor that boosted interest in this issue is the development of new methods for nucleic acid purification and separation based on the adhesion of nucleic acids to silica related to silica−phosphate interactions.[5] The latest achievements in nanoscale Si-based electronic technology open promising new avenues in the area of nucleic acid manipulation based on silica−phosphate interactions.

As shown, intermolecular hydrogen-bond formation in the DNA−silica contact layer is one of the major driving forces for DNA adsorption on silica surfaces.[6] IR studies indicate that hydrogen-bonded complexes between the phosphate groups of a DNA backbone and the silanols of a quartz surface prevail in interactions between DNA and quartz in vitro.[7] Once bonded, DNA can be damaged through a number of mechanisms that presumably involve the polarization abilities of the negatively charged silica surface and the hydrogen-bond formation and generation of hydroxyl radicals on the surface.[7] Such a strong interaction of the silica surface with the phosphate groups is used by living organisms for silica isolation once it gets inside the body: induced production of phospholipids in the lungs that coat silica particles is believed to be a protective reaction.[8] Another example of a silica−phosphate interaction in living systems can be found in the processes of bone growth.[9,10] It was shown both in vivo and in vitro that silica can act as a mineralizing agent for apatite[11,12] although the microscopic nature of this process remains unclear. It is believed that the crystallization of calcium phosphate is induced by the accumulation of calcium and phosphate ions on the silica surface. The calcium cations get attracted to the negatively charged silica surface, and the phosphate anions form hydrogen bonds with the silanol hydroxyls.

Despite the utmost importance of phosphate adsorption on the silica surface, to the best of our knowledge there are not any theoretical calculations concerning this phenomenon. The purpose of this research is to characterize silica−phosphate complexes, the strength of binding, the geometry and charge

10.1021/jp981996r CCC: $18.00
Published on Web 02/13/1999

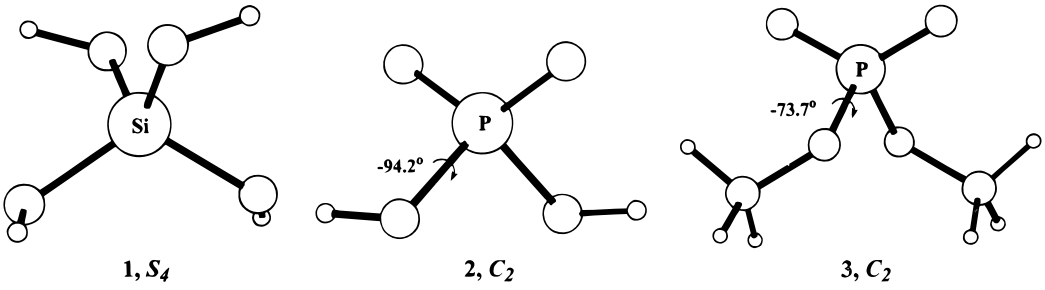

Figure 1. Isolated clusters: $Si(OH)_4$ (**1**), $H_2PO_4^-$ (**2**), and $(CH_3O)_2PO_2^-$ (**3**).

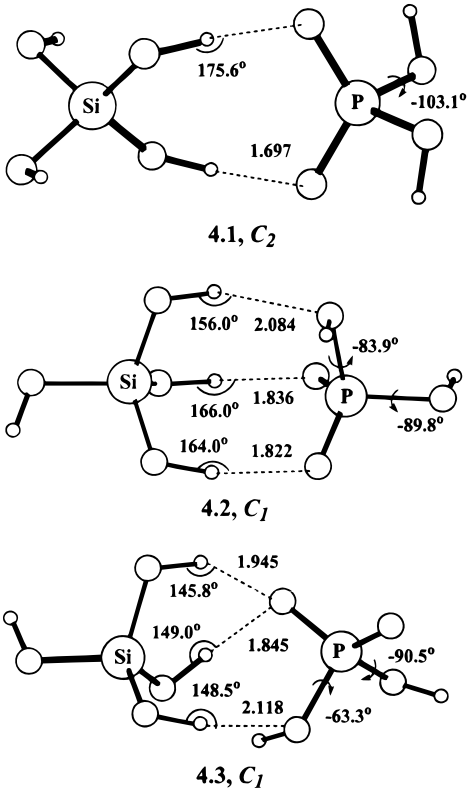

Figure 2. Hydrogen-bond complexes $Si(OH)_4-H_2PO_4^-$ (**4**).

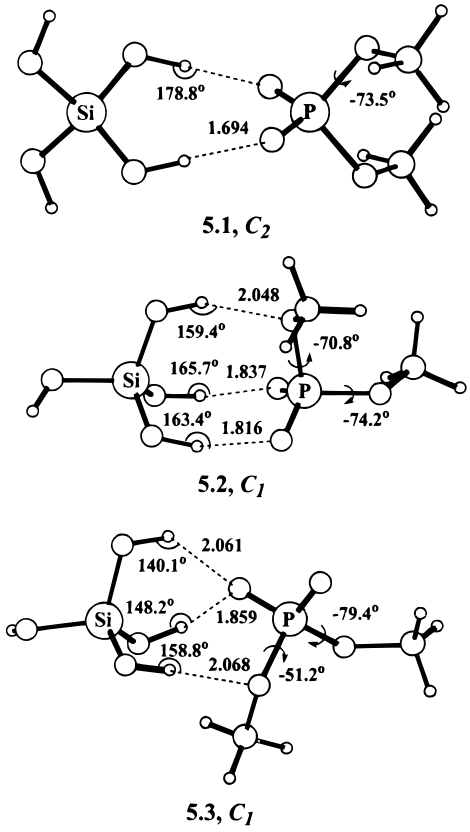

Figure 3. Hydrogen-bond complexes $Si(OH)_4-(CH_3O)_2PO_2^-$ (**5**).

distribution changes, and the IR spectra alterations accompanying adsorption in vacuo and in aqueous solutions which will be helpful in identifying such changes in real systems. This study does complement our earlier investigations of model phosphorus systems[13] and the recent predictions on interactions of DNA bases.[14]

2. Calculations

The first principle density functional (DFT) theory calculations using the GAUSSIAN-92 package of programs[15] were carried out on orthosilicic acid, $Si(OH)_4$ (**1**), the dihydrogen phosphate (DHP) anion, $H_2PO_4^-$ (**2**), the dimethyl phosphate (DMP) anion, $(CH_3O)_2PO_2^-$ (**3**) (Figure 1), and hydrogen-bond complexes between **1** and **2** to yield complex **4** (Figure 2) and between **1** and **3** to yield complex **5** (Figure 3). Additionally, doubly hydrogen-bonded monohydrated complexes of $Si(OH)_4$ (**6**), $H_2PO_4^-$ (**7**), and $(CH_3O)_2PO_2^-$ (**8.1**) (Figure 4) and the dihydrated complexes of $(CH_3O)_2PO_2^-$ (**8.2** and **8.3**) (Figure 5) were considered in order to evaluate the changes in the geometries, charge distributions, and IR spectra associated with phosphate adsorption on silica in the presence of water. Also, complexes of DHP and DMP with a sodium cation, symmetric **9** and **10.1** and asymmetric **10.2** (Figure 6), were investigated to compare the results with experimental data on crystalline salts. Initially all isolated clusters were optimized at the HF level using the 3-21+G(d) split-valence basis set with d-type polarization functions and diffuse functions added to the basis set of Si and P[16] with geometries reported for the global minima, viz. for **1** S_4 symmetry,[17,18] for **2** and **3** C_2 symmetry.[19,20] The minimum-energy clusters were further reoptimized using the B3LYP Becke three-parameter correction to exchange, combined with the Lee−Yang−Parr correction to the local correlation potential.[21] The B3LYP calculations were performed in conjunction with the 6-31+G(d,p) split-valence basis set with added polarization p-functions for H and d-functions for Si, P, O, and C. Additional diffuse functions were added to the basis set for the heavy atoms. It was shown elsewhere[22,23] that both the geometries and IR spectra of hydrogen-bonded complexes obtained in the DFT and MP2 calculations with this basis set are similar and within 1%, except for the very sensitive C(H)-OPO torsion and C−O−P phosphoester angles which can differ by as much as 5%. The calculations were performed with the Int=FineGrid option. Optimized geometries were confirmed as minimum-energy structures without imaginary frequencies. In the present study, the phosphate clusters, both isolated and

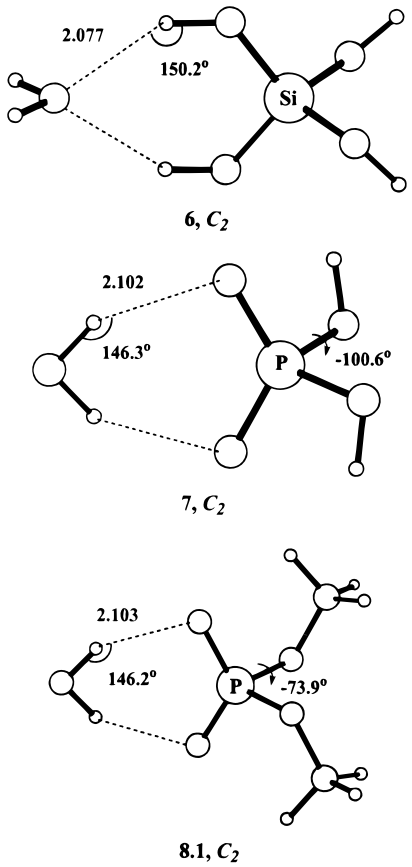

Figure 4. Monohydrated clusters: $Si(OH)_4-H_2O$ (**6**), $H_2PO_4^- - H_2O$ (**7**), and $(CH_3O)_2PO_2^- - H_2O$ (**8.1**).

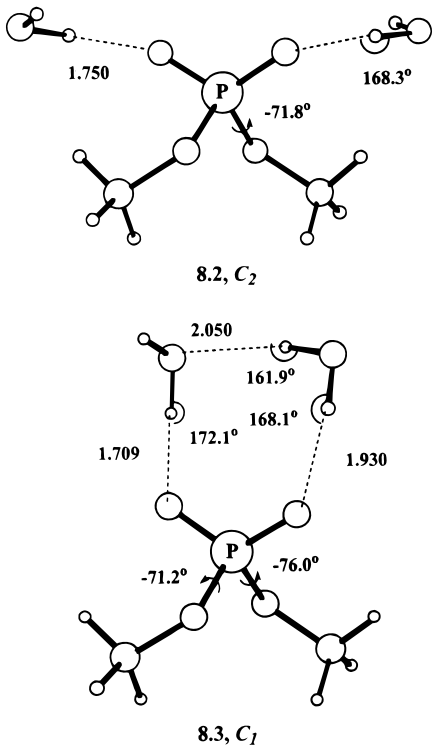

Figure 5. Dihydrated clusters: symmetric $(CH_3O)_2PO_2^- - 2H_2O$ (**8.2**) and asymmetric cyclic (**8.3**).

hydrogen bonded, were considered with the *-sc/-sc* (in the description of torsion angles the IUPAC−IUB approved nomenclature with *s* standing for *syn*, *a* for *anti*, *c* for *clinal*, and *p* for *periplanar* is used)[24] torsion angles (or the marginal *-ac/-ac* torsion angles describing the minimum-energy isomer of the dihydrogen phosphate anion) mimicking the fragments of a phosphate-sugar backbone of a right-handed nucleic acid helix. The effects of complexation on the relative energies of the phosphodiester backbone conformations were estimated by comparing the compact *-sc/-sc* conformations with the half-extended *-sc/ap* conformations (also fully optimized). The basis-set superposition error (BSSE) was estimated by the counterpoise method.[25] The atomic charges were estimated using the Mulliken charge partitioning scheme.[26]

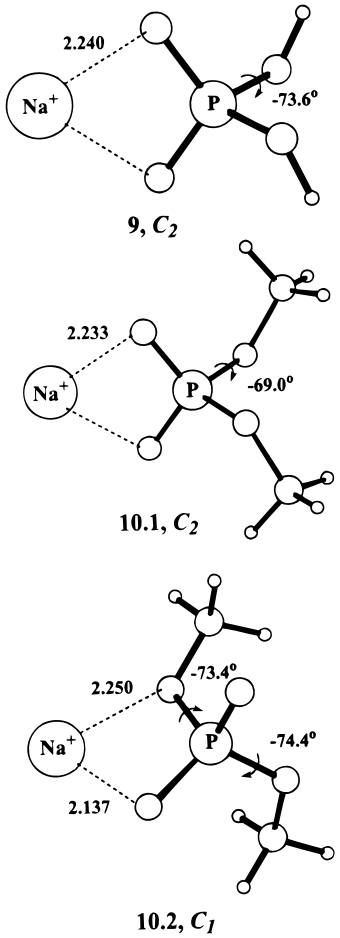

Figure 6. Phosphate complexes with sodium cation: symmetric $H_2PO_4^- Na^+$ (**9**) and $(CH_3O)_2PO_2^- Na^+$ (**10.1**) and asymmetric $(CH_3O)_2PO_2^- Na^+$ (**10.2**).

3. Silica and Phosphate Species in Vacuo, in Complex with Sodium Cation, and in Monohydrated Forms

In neutral or slightly basic solutions the silanol groups of the silica surface are partly deprotonated due to the weak acidity of these groups with a reported average pK_a ranging from 6.8 to 7.1.[27,28] As a result, the silica surface in aqueous solutions bears a negative charge which repels the anionic phosphate groups. It is not surprising that the presence of cations in solution, which are attracted by the negatively charged silica surface and phosphate groups, thereby neutralizing the negative charge, enhances the formation of silica−phosphate complexes. For example, adsorption of DNA on the silica surface was shown to be promoted by the presence of strong electrolytes (such as sodium salts) and was connected to the dehydration of DNA and silica surfaces and to the shielding effect of ions.[6] The higher acidity of the protonated forms of phosphates (e.g., $pK_{a1}(H_3PO_4) = 2.12$)[29] than that of silanols suggests that the

TABLE 1: Geometries and Net Atomic Charges of Orthosilicic Acid and Dihydrogen Phosphate (DHP) and Dimethyl Phosphate Anions Optimized at the B3LYP/6-31+G(d,p) Level

	orthosilicic acid[a]		
parameter	$Si(OH)_4$	$Si(OH)_4-H_2O$	$Si(OH)_4-H_2PO_4^-$
	Bonds (Å)		
Si−O	1.650	1.657	1.671
Si−O(H-b)		1.649	1.640
O−H	0.964	0.964	0.964
O−H(H-b)		0.968	0.995
H···O		2.077	1.697
	Angles (deg)		
O−Si−O1	106.2	109.4	102.9
O−Si−O2(or H-b)	116.2	111.8	114.3
Si−O−H	117.1	116.4	111.0
Si−O−H(H-b)		115.7	120.2
O−H···O		150.2	175.6
	Charges (au)		
Si	2.058	2.028	2.119
O	−0.888	−0.849	−0.934
O(H-b)		−0.928	−1.001
H	0.373	0.362	0.353
H(H-b)		0.412	0.471
$Si(OH)_4$	0	−0.020	−0.102
	Electron Overlap Populations		
Si−O	0.089	0.060	−0.115
Si−O(H-b)		0.079	0.167
H−O	0.245	0.252	0.232
H−O(H-b)		0.237	0.223
H···O		−0.006	0.028

	dihydrogen phosphate and dimethyl phosphate[b]								
	in vacuo		H_2O		$Si(OH)_4$		Na^+		exp[48] Ba^{2+}
parameter	DHP	DMP	DHP	DMP	DHP	DMP	DHP	DMP	DMP
				Bonds (Å)					
P−O	1.682	1.683	1.668	1.669	1.655	1.656	1.636	1.631	1.61
P═O	1.507	1.504	1.512	1.508	1.514	1.511	1.521	1.523	1.52
C/H−O	0.967	1.419	0.967	1.422	0.967	1.426	0.968	1.436	1.46
$H/Na^+\cdots O$			2.102	2.103	1.697	1.694	2.240	2.233	
				Angles (deg)					
O−P−O	100.9	99.5	101.3	100.3	101.9	101.4	103.6	103.6	103.5
O−P═O1	106.4	105.6	106.8	106.2	106.8	106.4	107.9	107.9	
O−P═O2	107.1	108.8	108.4	109.5	108.8	109.4	111.3	111.7	
O═P═O	126.0	125.5	123.1	122.9	122.0	122.0	114.3	113.7	121.6
C−O−P	105.7	117.3	106.3	117.5	107.2	117.9	110.9	118.7	117.0
C/HOPO	−94.2	−73.7	−100.6	−73.9	−103.1	−73.5	−73.6	−69.0	−69.9
O−H···O			146.3	146.2	175.6	175.8			
				Charges (au)					
P	1.696	1.979	1.737	1.998	1.843	2.094	1.816	2.106	
O(═P)	−0.898	−0.910	−0.944	−0.956	−0.968	−0.985	−0.936	−0.976	
O(−P)	−0.791	−0.668	−0.764	−0.644	−0.761	−0.642	−0.738	−0.640	
C/H	0.341	−0.285	0.348	−0.283	0.358	−0.276	0.369	−0.283	
DHP/DMP	−1	−1	−0.984	−0.988	−0.898	−0.895	−0.796	−0.783	
				Electron Overlap Populations					
P═O	0.385	0.398	0.380	0.387	0.348	0.345	0.270	0.248	
P−O	−0.037	−0.040	−0.029	−0.026	0.007	0.037	0.032	0.043	
C−O	0.208	0.028	0.212	0.034	0.217	0.018	0.219	0.041	
$H/Na^+\cdots O$			0.013	0.016	0.028	0.033	0.075	0.087	

[a] Isolated, in doubly hydrogen-bond complexes with a water molecule and the DHP anion. [b] In vacuo, in doubly hydrogen-bond complexes with a water molecule and orthosilicic acid.

phosphate moieties, deprotonated in near-neutral solutions, act as hydrogen acceptors during the formation of hydrogen-bonded complexes with the silanols of the silica surface while the silanols contribute hydrogens to the hydrogen bonds. The smallest molecular unit mimicking the silanol groups of the silica surface and the [SiO_4] tetrahedron (the structural unit of silica frameworks) is orthosilicic acid, $Si(OH)_4$. In addition, this acid and its deprotonated forms are abundant in natural aqueous solutions[30] and present in trace amounts in biological fluids. These considerations and the modest size of this molecule are accountable for an extensive list of theoretical calculations performed on orthosilicic acid, **1**, at different levels of theory.[17,31,32] As well, the adsorption of water and other small organic and inorganic molecules on the silica surface was studied mainly using orthosilicic acid, $Si(OH)_4$, to model the surface silanol groups.[33,34] This approach is employed in the present study to model the adsorption of phosphates. Figure 1 depicts the minimum-energy configuration of orthosilicic acid, and Table 1 lists the optimized geometries and charges of orthosilicic acid. The energies of the stable isomers are listed in Table 2.

Phosphoric acid and its substituted derivatives, such as the phosphate esters and diesters of nucleic acids and phospholipids,

TABLE 2: Total, Zero-Point (ZPE) and Stabilization Energies (SE, ZPE correction not included) of the Optimized Silica−Phosphate Clusters at the B3LYP/6-31+G(d,p) Level[a]

species	no.	*E* (hartrees)	ZPE (kcal/mol)	SE (kcal/mol)
$Si(OH)_4$	**1**, S_4	−593.01941	36.1(0)	
$H_2PO_4^-$	**2**, C_2	−643.64446	23.1(0)	
$(CH_3O)_2PO_2^-$	**3**, C_2	−722.24496	58.4(0)	
$Si(OH)_4-H_2PO_4^-$	**4.1**, C_2	−1236.71212	60.7(0)	-30(29)
	4.2, C_1	−1236.71260	61.5(0)	-31(28)
	4.3, C_1	−1236.70722		-27(25)
$Si(OH)_4-(CH_3O)_2PO_2^-$	**5.1**, C_2	−1315.31284	96.6(0)	−30(29)
	5.2, C_1	−1315.31366		−31(28)
	5.3, C_1	−1315.30587		−26(24)
$Si(OH)_4-H_2O$	**6.1**, C_2	−669.45992	51.3(1)	−4(3)
$H_2PO_4^- - H_2O$	**7.1**, C_2	−720.10433	38.7(0)	−16(15)
$(CH_3O)_2PO_2^- - H_2O$	**8.1**, C_2	−798.70478	74.3(0)	−16(15)
$(CH_3O)_2PO_2^- - 2H_2O$	**8.2**, C_2	−875.10133[b]	90.5(0)	−35(25)[b]
	8.3, C_1	−875.16283	90.1(0)	
$Na^+-H_2PO_4^-$	**9**, C_2	−805.94223	24.2(0)	
$Na^+-(CH_3O)_2PO_2^-$	**10.1**, C_2	−884.54524	60.0(0)	
	10.2, C_1[c]	−884.53517	59.9(0)	
H_2O		−76.43405	13.4(0)	

[a] Number of imaginary frequencies are given in parentheses following ZPE's. BSSE-corrected values are given in parentheses following SE's of hydrogen-bond complexes. [b] At the B3LYP/6-31G(d,p) level. [c] Asymmetric Na^+ position.

are strong acids. This is why, in near-neutral solutions of living cells, these phosphate groups are deprotonated and why most theoretical studies are concerned with phosphate anions[35,36] (in modeling of crystalline salts the fully protonated phosphate cation, $P(OH)_4+$, is often considered to mimic the $[PO_4]$ tetrahedra[37]). The dimethyl-substituted derivative of the dihydrogen phosphate anion, which mimics the functional group of the nucleic acid backbone and the anionic head of the phospholipids, was thoroughly investigated.[38] Isomers of 2-fold axial symmetry with torsion angles in the *sc/sc* sector which coincide with the torsion angles found in the phosphate diesters of the nucleic acid helix were shown to be global minima for both the DHP and DMP anions (see Figure 1). The anomeric effect (negative hyperconjugation)[39] is believed to be responsible for stabilization of phosphate moieties in this compact conformation.

The results of the geometry optimization of the DHP and DMP anions at the B3LYP/6-31+(d,p) level are in a good agreement with previous theoretical studies[40] and compare favorably with the experimental crystallographic data on dihydrogen and dimethyl phosphate salts.[41−43] Some deviation in the geometries, viz. shorter bonds and smaller phosphinyl and larger phosphodiester angles observed in the crystalline salts (there is no experimental data of the geometries of investigated clusters in vacuo or in solutions), can be related to the effect of the crystal field, the presence of water molecules in the crystalline salts, and a general trend of calculations accounting for electron correlation to overestimate bond lengths.[44]

To investigate the effects of the complexation of phosphate anions by a countercation, we performed calculations on the DHP and DMP complexes with a sodium cation (complexes **9** and **10**, respectively, see Figure 6). While experimental studies of the phosphate salts suggest a preference of sodium cations to occupy a nonplanar position around the anionic oxygens,[45] theoretical calculations place the sodium cation on the line bisecting the phosphinyl triangle[46] (this configuration was shown to be competitive also in water solutions[35]). The changes in the geometries of the phosphate groups occurring during coordination by the sodium cation are in accordance with recently reported calculations.[47] As expected, our calculations (see Table 1) on the symmetric DHP and DMP complexes with a sodium cation (complexes **9** and **10.1**, respectively) indicate significant improvement in the reproduction of the phosphate geometry experimentally observed in crystalline barium diethyl phosphate[48] compared to the anion in vacuo: the P−O bond (in this report double bonds are used to show phosphinyl oxygens and single bonds to show ester or hydroxyl oxygens) becomes shorter compared to the isolated DMP and approaches the experimental finding; the P═O and the C−O bonds lengthen, the O−P−O and the C−O−P angles increase, and the COPO torsion angle decreases. The only parameter that deviates further from the crystallographic value upon complexation by the sodium cation is the O═P═O angle, decreasing below the experimental value. One explanation for this discrepancy can be the preferential location of a sodium cation in a nonsymmetrical position outside the phosphinyl plane in crystalline salts (stabilization of countercations in these positions can be related to the coordination of both the cation and the anion by water molecules incorporated into the crystalline structure). In fact, our calculations of the asymmetric complex (**10.2**) with a sodium cation occupying a nonplanar position between the anionic and ester oxygens (the angle between the $Na^+\cdots O-P$ and the $(Na^+)O-P=O$ planes is 12°, see Figure 6) suggest that the phosphinyl angle decreases to 124.9° and approaches the value observed in the experiment. At the same time, the C−O, P−O, and P═O bonds of one-half of the phosphate group solvated by a sodium cation elongate and vice versa. These bond length alterations can be related to a redistribution of electron density and pertinent changes in the character of bonding, namely, enhanced negative hyperconjugation lengthens the ester P−O bonds and widen the O−P−O diester angles, and electrostatic effects leading to the contraction of radii of less electronegative atoms have an opposing effect on the bond lengths. This isomer (**10.2**) is a local minimum, having 6.3 kcal/mol higher total energy than the symmetric complex (**10.1**). The calculated geometry of the sodium complex with DHP correlates well with the low-temperature data for the crystalline KH_2PO_4 salt.[49]

Coordination of the phosphate groups by a sodium cation results in the condensation of the mobile π-electron density of the phosphinyl bonding on the anionic oxygens, thereby reducing the partial double-bond character and increasing the negative charges on the anionic oxygens and the positive charge on phosphorus. In turn, these changes can enhance back-donation of *p*-electron density of the ester oxygens to the phosphorus atom. Increased repulsion between π-electron densities around the phosphoester bonding, as well as the reduction of the anomeric effect, can be responsible for further deviation of the C(H)OPO torsion angles from the optimum angle. Similarly, both back-donation and the less-effective anomeric effect can result in strengthening of the P−O bonds, which is indicated by an increase in the electron overlap densities and the shortening of these bonds. Further studies are necessary to separate contributions of these effects to the changes in the geometries of the DHP and DMP anions. Despite the drastic reduction of negative hyperconjugation, earlier calculations[47] suggest stabilization of the *-sc/-sc* conformation upon complexation by a sodium cation, viz. the partially extended *-sc/ap* conformation in the coordinated form is less stable by 1.3 kcal/mol while in vacuo this conformation is only 1.0 kcal/mol higher in energy (at the MP2/6-31G(d) level). It is possible that a reduction of the overall negative charge on the phosphate anion through its transfer to the sodium cation diminishes the energetic advantages of distributing this charge over the extended structures with the backbone torsion angles in the *ap* sector. Indeed, calculations performed in this study indicate a charge

TABLE 3: Characteristic Bands in Spectra of DHP and DMP Isomers in Vacuo, in Complex with a Water Molecule, with a Sodium Cation, and with Orthosilicic Acid Calculated at the B3LYP/6-31+G(d,p) Level[a]

band assignment	in vacuo		Na^+ symmetric		Na^+ asymmetric	H_2O monohydrated		H_2O dihydrated	$Si(OH)_4$		exp[40] Na^{2+}
	DHP	DMP	DHP	DMP	DMP	DHP	DMP	DMP	DHP	DMP	DMP
						DHP/DMP					
*ss*P−O	732(128)	675(103)	803(75)	730(33)	642(238)	752(124)	692(104)	698(94)	769(109)	703(122)	755
*as*P−O	762(371)	698(327)	862(310)	795(245)	754(175)	796(450)	735(481)	748(458)	815(240)	746(227)	807
*as*C−O		1079(220)		1063(263)	1063(92)		1075(233)	1077(242)		1074(249)	1042
*ss*C−O		1095(22)		1069(39)	1087(190)		1090(37)	1093(40)		1088(43)	1065
*ss*P═O	1065(254)	1067(328)	1093(227)	1082(451)	1047(341)	1068(334)	1065(392)	1068(473)	1072(394)	1066(458)	1116
*as*P═O	1290(387)	1279(326)	1209(380)	1174(273)	1294(388)	1266(325)	1249(275)	1250(334)	1251(412)	1233(359)	1244

[a] Frequencies, ν, in cm^{-1} followed by intensities, I, in km/mol given in parentheses.

transfer between the ions in the sodium-phosphate pair, reducing the unitary charge partitioning to 0.8 au (according to the Mulliken partitioning scheme). It is also possible that the back-donation can contribute to the stabilization of the NaDMP phosphodiester backbone in the compact conformation. The overall effect of the complexation of DMP by a sodium cation, as found in this study, results in a relative destabilization of the *-sc/-sc* conformation with respect to the one: the energy difference is reduced from 1.1 kcal/mol for DMP in vacuo (torsion angles of the *-sc/ap* conformation are −71.4°/164.8°) to 0.5 kcal/mol for its complex with Na^+ (torsion angles are −64.3°/173.6°).

The harmonic vibrational frequencies and intensities of the isolated molecules (orthosilicic acid, the DHP and DMP anions) obtained in this study correlate well with those reported previously in numerous studies.[17,31,40,50,51] A number of main IR-active bands are listed in Table 3. The assignment of the characteristic bands is given according to the major contributor to the potential energy of vibration. No experimental spectroscopic data have been reported for either DHP or DMP anions in vacuo, and therefore, a comparison can only be made with either the solid-state or solution spectra. Notably, ab initio calculations predict lower band frequencies due to the P−O stretching modes and higher frequencies of the C−O stretching bands, especially for the P═O asymmetric vibration, which is related to the crystal-field effect and its effect on the bond lengths.[20] We investigated the effect of complexation of the phosphate anions by a sodium cation on the IR spectra of phosphates. Indeed, the calculated frequencies of the characteristic bands match the experimental values much better (see Table 3). Further improvement can be achieved by scaling.[52] The only exception is underestimation of the *as*P═O frequency in the calculations. This stretching mode is extremely sensitive to the local environment; thus, the discrepancies can be related to the differences between that in vacuo and in a crystal, e.g., the crystal-field effect and the preferential location of sodium cations in asymmetric positions between the phosphinyl and the ester oxygens in crystalline salts. Asymmetric coordination of the phosphate groups by the sodium cation leads to asymmetric alterations of bond lengths (vide supra) and, consequently, to a partial decoupling of the stretching vibrations of the affected bonds. In fact, our calculations of DMP coordinated by a sodium cation occupying a nonplanar position between the anionic and ester oxygens (**10.2)** indicate a blue shift of the band dominated by vibrations of the phosphinyl bonding which is not solvated by the sodium cation with respect to the *as*P═O band of both the DMP anion in vacuo and its symmetric Na^+ complex (see Table 3). In contrast, the band due to the phosphoester bonding of the unsolvated half of the phosphate moiety is characterized by a frequency lower than the *as*P−O stretch of DMP in the symmetric sodium complex. At the same time, the bands dominated by vibrations of the phosphinyl P═O bond and the phosphoester P−O bond that are solvated by the sodium cation undergo a red shift relative to the symmetric stretching of the corresponding bonds in both environments. The C−O stretching vibrations reverse the order of their intensities, i.e., the asymmetric stretch is less intense than the symmetric one. The band due to the C−O bond of the solvated half of the phosphate group is characterized by a frequency of the *as*C−O stretch of DMP in the symmetric sodium complex, while the mode of the other C−O bond corresponds to a higher frequency than the frequency of the *ss*C−O stretch (see Table 3).

Formation of the symmetric complex with the sodium cation does not significantly affect the frequency of the *ss*P═O stretching mode: it remains in a lower frequency range. Due to the red shift of the C−O vibrational frequencies, this band now lies in a higher frequency range, in accordance with experiment.[53] In all of the other complexes, calculations yield a reverse order in line with high-level calculations reported earlier (with a basis set extended beyond 3-21G(d)).[50,51] Invariance of the symmetric P═O stretch, which is coupled strongly with the symmetric P−O stretch, toward the presence of a cation affecting the bond lengths is likely due to the cancellation of the two opposing effects: a lengthening of the P═O bond, reducing the bond force constant, and a shortening of the P−O bond, raising the bond force constant.

Monohydrated orthosilicic acid with an acid molecule acting as a single hydrogen-bond donor was shown to exist in a number of stable isomers.[54] In this study, for adequate comparison with silica−phosphate complexes **4** and **5**, it was necessary to optimize complex **6** with the oxygen of water forming bifurcated bonds with two hydrogens of orthosilicic acid. All other minimum-energy monohydrated and dihydrated complexes found in this study were "contaminated" by hydrogen bonds with the silanol groups accepting hydrogen. Such hydrogen bonds are not present in the silica−phosphate complexes under consideration. The monohydrated bifurcated complex of orthosilicic acid (**6**) is given in Figure 4. The axial symmetry C_2 complex is found to be a transition-state structure connecting two symmetric global-minimum cyclic structures with the water molecule bridging two hydroxyls of orthosilicic acid[34] (at the MP2 level of calculations, this complex is a local minimum[23]).

The stabilization energies (SE) along with the BSSE corrected values are listed in Table 2. As shown, the BSSE correction significantly improves the reproducibility of the experimentally observed stabilization energies of the hydrogen-bonded complexes obtained by the DFT calculations employing the B3LYP functional and double-ζ basis set.[55] Thus, for water dimer it was shown that the BSSE corrected stabilization energies were within 0.2 kcal/mol of experimental values, which is less than the experimental uncertainty of measurements. The bifurcated C_2 complex (**6**) has a fairly low stabilization energy (see Table

2) of around −3 kcal/mol after the BSSE correction compared with approximately −7 kcal/mol found for the lowest energy monohydrated complex.[34] Therefore, due to this low stabilization energy, only a small fraction of neighboring silanol hydroxyls can be expected to form bifurcated complexes with water molecules in real systems at ambient conditions, and this complex is used in this study solely to investigate the trends in the changes of the silanol geometry and the stretching vibrations occurring upon phosphate adsorption in aqueous solutions. The weakness of the hydrogen bonds in this complex comes from the unfavorable geometry of the complex. The hydrogen-bond angles, O···H−O, deviate significantly from the optimal angle value close to 180°. Thus, it is as low as 150° and is accompanied by a rather long hydrogen bond of ca. 2.08 Å (see Table 1).

Hydration of orthosilicic acid results in a redistribution of the electron density: hydroxyls not participating in hydrogen-bond formation become less polarized and less strongly bonded to the silicon atom (inferred from the lengthening of the Si−O bonds and reduction of the electron overlap density, see Table 1). Adversely, the participating hydroxyls become polarized to a larger extent and bonded more strongly to the silicon atom.

One of the parameters describing the distortion of the tetrahedral groups [TO_4], where atom T is coordinated by four oxygen atoms, is the sum of the six OTO angles. In a regular tetrahedron the sum is 656.82°. Maximum separation of the atoms occupying the tetrahedral apexes is provided in a regular tetrahedron. Thus, the deviation of this sum from that of the ideal tetrahedron can be an indication of the prevalence of the repulsive interactions between apex atoms. Hydration of orthosilicic acid with the bifurcated geometry of the complex does not change the average charge on the oxygen atoms and consequently does not affect the distortion of the [SiO_4] tetrahedron, i.e. the sum remains at 657.2°.

The sum of all the T−O bonds of the [TO_4] tetrahedra can be another characteristic parameter describing the tetrahedral geometry. Monohydration of orthosilicic acid results in an overall lengthening of the Si−O bonds: the sum increases by 0.01 Å.

The lowest energy monohydrated singly deprotonated phosphates arguably have an axial symmetric geometry of the hydrogen-bonded complex with a water molecule bridging the phosphinyl oxygens with stabilization energies between −20 and −28 kcal/mol depending on the level of calculations (without the BSSE correction).[19,56−58] The multihydrated phosphate groups were shown to contain mainly water molecules lying in the exterior of the phosphinyl triangle and singly hydrogen bonded to anionic oxygens.[59] In accordance with previous studies, optimizations of the monohydrated phosphate species (**7** and **8.1**) (see Figure 4) performed in this work yielded complexes with axial C_2 point-group symmetry as zero-order minima on the potential-energy surface. These complexes are characterized by stabilization energies of around −15 kcal/mol after the BSSE correction (good correlation between noncorrected values and the previously reported ones is found), which are given in Table 2. Significant negative charges on the phosphinyl oxygens of the phosphate anions suggest a more effective Coulombic interaction and, therefore, lessened directionality of hydrogen bonding. Consequently, although hydrogen bonding in the monohydrated phosphate complexes is geometrically less favorable (see Table 1b) compared with that in the monohydrated bifurcated orthosilicic acid (hydrogen bonds are longer and hydrogen bond angles are smaller), the former is stronger. The geometric and energetic characteristics of hydrogen bonding in the monohydrated DHP and DMP anions are identical within the uncertainty of the calculations.

In the studies of the crystalline phosphates, distortion of the phosphate tetrahedra was correlated with the hydrogen-bond formation.[60−62] Indeed, our study suggests that upon monohydration of the phosphate group, the phosphate tetrahedra become less deformed (the sum of the angles increases from 654.0° to 654.7° for the dihydrogen phosphate anion and from 653.6° to 654.5° for the dimethyl phosphate anion, approaching the ideal tetrahedron limit). Most likely, such an observation is associated with the decrease of the double-bond character of the phosphinyl bonds, reducing the O═P═O angle and the back-donation of *p*-electrons of the ester oxygens to the phosphorus atom, widening the phosphodiester O−P−O angle (see Table 1b). In phosphate anions equipoised by a sodium cation, these effects are even larger and the [PO_4] tetrahedra are less deformed (the sum of the angles is 656.3° in Na^+−DHP and 656.5° in Na^+−DMP). The HOPO torsion angle of the DHP anion phosphohydroxy backbone increases, in full accordance with a reduction in the negative charges on the phosphate hydroxyl oxygens (vide infra) accompanied by the reduction of the anomeric effect. The COPO torsion angle of the DMP anion backbone increases slightly as well. Such an alteration can be related to the onset of the magnified repulsion between the increasingly positively charged methyl groups, compensating the reduction of the anomeric effect.

The sum of all the phosphorus−oxygen bonds is used as another characteristic parameter describing the phosphate groups.[63,64] The experimentally observed value of 6.184 Å for the monodeprotonated phosphates[63] is very close to those found in phosphates with organic substituents, viz. 6.160 Å.[47] At the same time, the bond parameters found in the phosphate groups of the DNA backbone agree well with those found in the phosphate groups containing organic substituents.[65] In this study, the hydration of the dihydrogen phosphate anion results in an increase of the P═O bond lengths and a shortening of the P−O bonds while the sum of the oxygen−phosphorus bond lengths decreases upon monohydration from 6.378 to 6.360 Å. As a result of complexation by the sodium cation, the sum becomes even closer to the values found in experiments, viz. it constitues 6.314 Å. Almost identical changes are observed for the dimethyl phosphate anion: the sum of the bond lengths decreases from 6.374 to 6.354 Å upon monohydration and to 6.308 Å during complexation by the sodium cation. The sum of all the oxygen−phosphorus bond lengths could be used as an indication of the effectiveness of negative hyperconjugation within the phosphodiester linkage and/or a measure of the total effective charge on a phosphate moiety.

Hydration of phosphate anions gives rise to an increase in the polarization of the phosphinyl bonds, which is indicated by the increased charge separation (see Table 1) and results in a better alignment of the phosphate hydroxyls along the 2-fold axis of the molecule. The calculated negative charges on the anionic oxygens increase upon formation of the hydrogen-bonded complexes, while the negative charges on the ester oxygens decrease. The virtually unchanged total charge on the phosphate anions (see Table 1) implies the absence of a substantial charge transfer to a water molecule. Consequently, in contrast to complexation by the sodium cation, where weakening of the anomeric effect is at least partially compensated by the reduction of the advantages of charge distribution over extended structures, hydration results in a destabilization of the compact *-sc/-sc* conformation through reduction of the anomeric effect (in accord with experimental studies),[66] viz. the

difference in total energies of the *-sc/-sc* and *-sc/ap* (−72.0°/172.0°) conformations is only 0.4 kcal/mol.

Consistent with its effect on the geometries, monohydration of the DHP anion results in a blue shift of the *ss*P−O band by 20 cm^{-1} and of the *as*P−O band by 34 cm^{-1} and in a red shift of the *as*P═O stretching mode by 24 cm^{-1}. Akin to the invariance of the *ss*P═O stretching mode to the presence of the sodium cation, monohydration increases its frequency by only 3 cm^{-1}. At the same time, the *ss*P−O and *as*P═O vibrations become less intense while the *as*P−O and *ss*P═O vibrations become more intense. As a result, *as*P−O becomes the most intense band (in vacuo *as*P═O is predicted to be the most intense band). These alterations in IR spectra are in good agreement with experimental studies, viz. a low-frequency shift of the intense *as*P═O band between 20 and 50 cm^{-1} and the virtual invariance of the *ss*P═O band are reported upon hydration of DNA fibers,[67,68] phosphate groups of phospholipids,[69,70] and phosphoesters.[71,72] Again, similar correlations are found in this study for the DMP anion. These calculations suggest red shifts for the *as*C−O and *ss*C−O bands by about 5 cm^{-1}, which compares reasonably with experimental ca. 10 cm^{-1} red shifts.[67]

The experimentally observed frequency shifts upon dissolution of crystalline sodium dimethyl phosphate salt[40] are in disagreement with these calculations based on a comparison of the symmetric monohydrated DMP and its complex with the sodium cation: the *as*C−O band shifts to a lower frequency by 4 cm^{-1} vs the calculated shift to a higher frequency by 12 cm^{-1}; the *ss*C−O band shifts to a lower frequency by 5 cm^{-1} vs the calculated shift to a higher frequency by 21 cm^{-1}; the *ss*P═O band shifts to a lower frequency by 32 cm^{-1} vs the calculated shift to a lower frequency range by 17 cm^{-1}; and the *as*P═O band shifts to a lower frequency by 36 cm^{-1} vs the calculated shift to a higher frequency range by 75 cm^{-1}. These discrepancies may result from a combination of the crystal-field effect in solid dimethyl phosphate salt and the effect of multihydration and coordination of DMP by sodium cations enduring dissolution in water. To estimate the former effect, we performed calculations on a dihydrated DMP anion. Geometry optimization at the B3LYP/6-31G(d,p) level (i.e., without diffuse functions, denoted hereafter as the DFT level to distinguish from the B3LYP/6-31G+(d,p) level), resulted in a minimum energy complex (**8.2)** with water molecules symmetrically coordinating the phosphinyl oxygens by single hydrogen bonds,[73] see Figure 5, with SE of −35 and −25 kcal/mol before and after the BSSE correction, respectively. Optimization at the B3LYP/6-31G+(d,p) level yields only an asymmetric cyclic triply hydrogen-bonded structure (**8.3**) with water molecules connected in a "head-to-tail" fashion and coordinating the phosphinyl oxygens. This complex is stabilized by the cooperative effect[74] and is lower in total energy by 3 kcal/mol (at the DFT level) than the symmetric (**8.2**) complex. Due to the presence of hydrogen bonding between water molecules, this complex (**8.3**) is not used further for energetic comparisons. Earlier results reported on the dihydration of DMP at the HF/3-21G(d) level (with water molecules symmetrically bridging the phosphinyl and ester oxygens)[50] suggest red shifts of *as*P−O and both of the C−O stretching bands and blue shifts of *ss*P−O and both of the P═O stretching bands upon addition of another water molecule to the coordination sphere of DMP. In this study, symmetric hydration of the DMP anion with another water molecule, complex **8.2**, assumes blue shifts of both P−O stretching bands and red shifts of the pairs of the P═O and C−O stretching bands, echoing the geometrical changes. At the same time, asymmetric dihydration, complex **8.3**, suggests blue shifts of all the major bands. As a result, the IR spectrum alterations correlate better with the experiment assuming symmetric coordination: the red shift of *ss*P═O is magnified while the blue shifts of *as*P═O and *as*C−O and the red shift of *ss*C−O are reduced. Further improvement in the reproduction of the experimental observation (except for the *ss*P═O band) is achieved by considering the IR vibrational spectrum of the asymmetric sodium-phosphate complex (**10.2)**. Thus, at the DFT level, the calculated alterations of the IR spectrum upon dissolution of NaDMP in water (comparing the spectra of **8.2** and **10.2**) comprise a 9 cm^{-1} blue shift of the *as*C−O band, a 1 cm^{-1} red shift of the *ss*C−O band, a 23 cm^{-1} blue shift of the *ss*P═O band, and a 45 cm^{-1} red shift of the *as*P═O band.

4. Silica−Phosphate Complexes

4.1. Stabilization Energies of Complexes and Characterization of Hydrogen Bonding. Three minimum-energy silica complexes with the dihydrogen phosphate anion, found in this study, are depicted in Figure 2. The corresponding complexes of the methyl-substituted analogues are given in Figure 3. The total, zero-point vibrational, and stabilization energies are listed in Table 2. The silica−phosphate complexes with the largest stabilization energies of −29 kcal/mol for the dihydrogen (**4.1**) and dimethyl phosphate (**5.1**) anions have C_2 symmetry and are doubly hydrogen bonded. These stabilization energies indicate strong hydrogen bonding, comparable with that found in hydroxonium−water and hydroxyl−water complexes,[75] and exceed those found in the doubly hydrated complex (**8.2)** by ca. 2 kcal/mol per hydrogen bond (at the DFT level). Hydrogen-bond reinforcement occurring upon substitution of a water molecule by a molecule of orthosilicic acid in the complexes of the phosphate anions is also indicated by a doubling of the hydrogen-bond electron overlap densities (see Table 1). The geometrical characteristics of hydrogen bonding in the most stable symmetric complexes of DHP and DMP are very similar.

Interestingly, other isomers with torsion angles in the *-sc/-sc* sector found in this study and characterized by three hydrogen bonds have smaller stabilization energies. Complexes **4.2** and **5.2** have larger absolute values of total energies (see Table 2), but they also have larger zero-point vibrational energies and larger BSSE corrections. As a result, despite three hydrogen bonds (two hydrogen bonds formed with the phosphinyl oxygens and one with the hydroxy/ester oxygen), they have lower stabilization energies (see Table 2). Complexes **4.3** and **5.3** also have three hydrogen bonds: two bifurcated bonds with an anionic oxygen of the phosphate group and one hydrogen bond with an hydroxy/ester oxygen (see Figures 4 and 5) and have even lower SE's (see Table 2). The remarkable stability of the symmetric doubly hydrogen-bonded complexes arises from the perfect match between the geometries of orthosilicic acid and the phosphate anion, allowing for the formation of relaxed hydrogen bonding: the hydrogen bond angle is close to the optimal value. The silicon atom is displaced only slightly inside the undeformed oxygen tetrahedron. The formation of these complexes does not require a drastic change in the silanol hydroxyl orientation. These hydrogen bonds are very short—only around 1.70 Å. Due to such perfect arrangements for both hydrogen bonds in these complexes, the geometry of the Si−O−H···O═P chain and the energy of this hydrogen bond can reasonably approximate the most probable hydrogen-bond formation of a phosphate moiety, not only with geminal silanol hydroxyls but also with a singly hydroxylated silicon on the silica surface.

Hydrogen bonds in the lower symmetry complexes are more strained: the angles deviate significantly from linearity and are in the range between 160° and 165° for **4.2** and **5.2** (see Figures 2 and 3). The least stable complexes (**4.3** and **5.3**) have even more deformed hydrogen bonds, with the H···O−H angles between 140° and 160° (see Figures 2 and 3). Another destabilizing factor is related to the changes in the geometry of orthosilicic acid: the formation of three hydrogen bonds requires orientation of three hydroxyls of this molecule toward the phosphate group. This reorientation does not result in a noticeable deformation of the [SiO_4] tetrahedra due to the strong repulsion of the oxygen atoms bearing large negative charges. As a result of the strained geometry, the hydrogen bonds in triply bonded complexes are significantly longer, ranging from 1.82 to 2.08 Å for **4.2** and **5.2** and from 1.85 to 2.12 Å in **4.3** and **5.3** (see Figures 2 and 3).

4.2. Changes of Charge Distributions and Geometries upon Complex Formation. Upon formation of strong hydrogen-bond complexes with phosphate anions, orthosilicic acid experiences an intensification of the changes observed during its hydration (see Table 1). The geometries of this acid complexed with DHP and DMP are identical within the uncertainty of the calculations.

Similarly, the trends observed during the hydration of the phosphates are intensified upon their adsorption on the silica surface (see Table 1) and are related to both the more effective polarizing and the greater electron density abstracting abilities of orthosilicic acid compared to the water molecule. Reduction of the overall Mulliken charge on the phosphate anions to −0.90 au (see Table 1) indicates a noticeable transfer of electron density onto the silanols of orthosilicic acid.

The phosphinyl bonds become more polarized as a result of the phosphate adsorption on silica: both the positive charge on the phosphorus atom and the negative charge on the anionic oxygens increase. In fact, the charge separation in phosphinyl bonding in the silica−phosphate complexes is the highest among the complexes with three complexing agents: a water molecule, orthosilicic acid, and a sodium cation. Possibly due to the large positive charge on the phosphorus atom, the inductive charge transfer from the carbon atoms to the ester oxygens is most effective in the silica−phosphate complexes and results in the lowest electron overlap population of the C−O bonding (see Table 1). It is therefore possible that adsorption of phosphoester-containing species on a silica surface can promote their hydrolysis via the C−O ester bond cleavage. The reduced double-bond character of the phosphinyl bonding gives rise to its weakening and a decrease of the phosphinyl O═P═O angle. The phosphodiester O−P−O angle widens along with further enhancement of the back-donation by the ester oxygens. The anomeric effect weakens and is accompanied by strengthening of the P−O bonding. The changes in the tetrahedral angles sum up to a further reduction of the deformation of the phosphate tetrahedra, while the sum of the PO bonds decreases to around 6.33 Å. The C(H)OPO torsion angles deviate further from the optimal value: the HOPO angle opens to a greater extent while the COPO angle becomes smaller (see Table 1 and Figure 4). Thus, this observation suggests that adsorption of phosphates on silanol hydroxyls in aqueous solutions may have a destabilizing effect on the *-sc/-sc* conformation of the phosphodiester backbone, already weakened by hydration (vide supra), through reduction of the anomeric effect. In these calculations, the *-sc/ap* (−71.2°/174.3°) conformation of the phosphodiester backbone was found to be only 0.2 kcal/mol higher in energy than the *-sc/-sc* conformation. Therefore, at ambient conditions, thermal energy ($RT \approx 0.6$ kcal/mol) can induce a conformational change of the phosphate moieties adsorbed on the silanols.

TABLE 4: Changes in the Spectra of DHP and DMP Anions and Orthosilicic Acid[a] upon Adsorption Relative to their Spectra in Isolated and Monohydrated Forms[b] Calculated at the B3LYP/6-31+G(d,p) Level

band assignment	in vacuo	monohydrated	dihydrated sym	dihydrated asym	exp water[c]
		$H_2PO_4^-$			
*ss*P−O	37(0.85)	17(0.88)			
*as*P−O	53(0.64)	19(0.53)			
*ss*P═O	7(1.55)	4(1.18)			
*as*P═O	−39(1.06)	−15(1.26)			
		$(CH_3O)_2PO_2^-$			
*ss*P−O	28(1.18)	11(1.17)	0(1.82)	5(1.30)	
*as*P−O	48(0.69)	11(0.47)	4(0.76)	−2(0.50)	
*as*C−O	−5(1.13)	−1(1.07)	7(1.14)	−3(1.03)	2(1.46)
*ss*C−O	−7(1.95)	−2(1.16)	5(5.4)	−5(1.08)	
*ss*P═O	−1(1.40)	1(1.17)	2(1.08)	−2(0.97)	1(1.56)
*as*P═O	−46(1.1)	−16(1.31)	−16(0.7)	−17(1.07)	−3(1.5)
		$Si(OH)_4$			
*s*O−H					
DHP	−588(8.2)	−525(7.3)			
DMP	−599(8.9)	−536(8.0)			

[a] Frequency shift, $\Delta\nu$, in cm^{-1} followed by the ratio of intensities in parentheses. [b] Only major characteristic bands are shown. [c] Experimental observations are from ref 7 and reported for DNA adsorption on silica.

4.3. Changes in Infrared Spectra. The changes in the IR spectrum of the symmetric C_2 complexes (**4.1** and **5.1**) upon hydration and adsorption on silica are summarized in Table 4 along with the available experimental observations (see ref 7). During adsorption of the phosphate groups on silica in aqueous solutions, the following changes in the calculated IR spectra can be identified. (1) The *as*P═O band shifts to a lower frequency by 15 and 16 cm^{-1} for DHP and DMP, respectively, compared with the experimental 3 cm^{-1} red shift. (2) The *ss*P═O band shifts to a higher frequency by 4 and 1 cm^{-1} for DHP and DMP, respectively, compared with the experimental 1 cm^{-1} blue shift. (3) The *as*C−O band shifts to a lower frequency by 1 cm^{-1} compared with the experimental 3 cm^{-1} red shift in D_2O and 1 cm^{-1} blue shift in H_2O. (4) The ratio of the *ss*P═O band intensity to the *as*P═O one decreases from 1.03 to 0.96 for the DHP anion and from 1.43 to 1.28 for the DMP anion upon adsorption on silica while experiments suggest opposing alterations. (5) The ratio (*ss*P═O)/(*as*C−O) increases from 1.68 to 1.84 compared with the experimental rise from 1.56 to 3.46.

These observations (except for the experimentally observed increase of the *ss*P═O band IR activity with respect to that of the *as*P═O band) and changes in the band intensities are in good quantitative agreement with the experimentally detected changes in the IR spectra upon DNA adsorption on the silica surface (see Table 4).[7] Attenuation of the calculated ratios of intensities of the *ss*P═O and *as*P═O bands, contradicting the experimental observations, could be related to the effects of multihydration in addition to the coordination of the phosphate anions by a single silanol. The symmetric dihydrated complex of DMP, (**8.2**) has a lower ratio of intensity for these bands (0.94 at the DFT level) than its complex with orthosilicic acid (1.43 at the DFT level), and the *as*C−O band undergoes a 7 cm^{-1} blue shift upon formation of a silica−phosphate complex, in agreement with experiment. On the other hand, the ratio (*ss*P═O)/(*as*C−O) decreases from 1.77 to 1.68 upon complexation by orthosilicic acid, which contradicts the experimental observations. Differences in the spectra of the asymmetric dihydrated DMP and its symmetric complex with orthosilicic

acid are in disagreement with experimental observations (see Table 4). Therefore, the experimental alterations of the IR spectra of phosphoester moieties upon their adsorption on the silica surface seem to suggest that the changes in the geometries and charge distribution of these moieties during adsorption are in better correspondence with such changes occurring upon symmetric substitution of water molecules by orthosilicic acid in symmetric mono- and dihydrated complexes (**8.1** and **8.2**, respectively).

Changes in the ratios of the intensity of the P═O stretching bands consistent with experimental results are observed in the calculations at the HF/3-21G(d) level where the formation of hydrogen bond complexes results in the reduction of negative charges on the anionic oxygens. The experimentally observed attenuated red shift of the *as*P═O band can be possibly explained by the single coordination of the anionic $-PO_2^-$ groups by the silanol hydroxyls.

Alteration in the IR spectra during the formation of another silica−phosphate complex (**4.2**), viz. blue shifts for both *as*P═O and *ss*P═O by 7 and 6 cm^{-1}, respectively, accompanied by an increase in activity by 1.03 times for the former and a decrease by 0.78 for the latter, are in disagreement with experimental observations. Therefore, it is conceivable that formation of this type of hydrogen-bonded complex was not detected in the experiment, in accordance with its lower stabilization energy and the requirement of participation of three neighboring silanol hydroxyls.

Density functional theories have been shown to poorly reproduce the hydroxyl stretching frequencies, viz. underestimation of the O−H bonding and, as a result, low frequencies and large shifts upon formation of hydrogen bonding.[76,77] In addition, bands due to the stretching modes of the silica and phosphate hydroxyls are obscured by the IR activity of the water molecules. Hence, only the extremely intense stretching vibrational modes of the silanol hydroxyl are considered further in this report.

The most remarkable alteration of the silanol IR spectrum upon formation of the hydrogen-bond complex with phosphates is a drastic shift of the silanol hydroxyl (Si)OH stretching mode to a lower frequency region accompanied by a radical gain in IR activity (see Tables 3 and 4) found in the calculations of the symmetric complex (**4.1**). Specifically, the frequency of the stretching modes of the silanol hydroxyls acting as hydrogen donors is shifted to a lower range by almost 600 cm^{-1} with a 9-fold intensity gain relative to the spectrum of the molecule (**1**) in vacuo and by 540 cm^{-1} with an 8-fold intensity gain relative to the spectrum of the monohydrated acid (**6**) (see Table 4). Outstanding IR activity of the surface silanol hydroxyls participating in hydrogen bonding can be used to detect phosphate adsorption on the silica silanols. The calculated red shift of the vibrational frequency of the silanol hydroxyls upon formation of the bifurcated complex with a water molecule of 63 cm^{-1} is lower than the reported experimental value of 85 cm^{-1}.[78] Therefore, in the experimental studies of phosphate adsorption in aqueous solutions, a shift in the vibrational frequency of the silanol hydroxyls can be expected to be around 500 cm^{-1}.

5. Conclusions

This study implies formation of strong hydrogen-bonded complexes between the phosphates and the silanol groups of the silica surface with stabilization energies of around −14 kcal/mol per hydrogen bond. Hydrogen bonding in such complexes can be stronger than that in hydrated phosphates by ca. 2 kcal/mol. The effect of silica on molecules containing phosphate groups can be exerted by means of both polarization and electron density transfer. Silanols are found to induce the highest charge separation on the phosphinyl bonding of the phosphate groups among the three complexing agents considered, i.e., water, orthosilicic acid, and a sodium cation, with the electron density abstracting abilities second only to the sodium cation. The C−O ester bond of the DMP complex with orthosilicic acid is characterized by an unusually low electron overlap population, viz. less than in the DMP anion in vacuo and in the other considered complexes. For the DMP anion in vacuo in the series of the C_2-symmetry hydrogen-bonded complexes with water, orthosilicic acid, and a sodium cation, lengthening of the C−O and P═O bonds is observed. Along with it the anomeric effect is reduced, and the back-donation of *p*-electrons of ester oxygens to the phosphorus atom is enhanced. Both effects can be responsible for the shortening of the P−O bonds. At the same time, the phosphodiester backbone torsion angle proceeds through a maximum in the hydrated dimethyl phosphate anion and is minimal in the NaDMP. The stability of the compact *-sc/-sc* conformation of the phosphodiester linkage with respect to the extended *ap* conformations diminishes along with the reduction of the anomeric effect, reaching a minimum in the silica−phosphate complexes (the energy difference between the compact and extended conformations is only 0.2 kcal/mol). These observations indicate that adsorption of nucleic acids on a silica surface can have a destabilizing effect on the *-sc/-sc* conformation of the phosphodiester linkage. In the phosphate complex with the sodium cation, the energy difference between the compact and extended conformations was found to be higher than in the other investigated complexes.

The changes in the IR spectra upon adsorption of the phosphates calculated at the B3LYP/6-31+G(d,p) level on a silica surface are in close agreement with experimental results. The higher experimental frequencies of the symmetric P═O stretch compared to those of the C−O stretch were related to the complexation of phosphates by countercations. The significant overestimation in the red shift of the asymmetric P═O stretch and the opposing trend in the relative activities of the phosphinyl stretching modes upon phosphate adsorption on silica were related to the formation of singly hydrogen bonded phosphate complexes and multihydration. The IR band resulting from the stretching vibrations of the silica surface hydroxyls undergoes dramatic changes upon phosphate adsorption in aqueous solutions: it moves to a lower frequency range by about 500 cm^{-1} and becomes very intense with about an 8-fold intensity gain. This leads to a strong band at ∼3300 cm^{-1}, which can identify the formation of the hydrogen-bonded complexes of the phosphates on the silica surface.

Acknowledgment. The authors thank the Mississippi Center for Supercomputing Research for the computational facilities. This work was facilitated in part by NSF Grant No. OSR-9452857, the Office of Naval Research Grant No. N00014-95-1-0049, and the Army High Performance Computing Research Center under the auspices of the Department of the Army, Army Research Laboratory cooperative agreement No. DAAH04-95-2-0003/Contract No. DAAH04-95-C-0008, the content of which does not necessarily reflect the position or policy of the government, and no official endorsement should be inferred.

References and Notes

(1) Cairns-Smith, A. G.; Hartman, H. *Clay Minerals and the Origin of Life*; Cambridge University Press: Cambridge, 1986.

(2) Theng, B. K. G. *The Chemistry of Clay-Organic Reactions*; John Wiley & Sons: New York, 1974.

(3) White, D. H.; Kennedy, R. M.; Macklin, J. *Origin Life* **1984**, *14*, 273.
(4) Saffiotti, U.; Daniel, L. N.; Mao, Y.; Williams, A. O.; Kaighn, M. E.; Ahmed, N. *Rev. Mineral.* **1993**, *28*, 523.
(5) Boom, R.; Sol, C. J. A.; Salimans, M. M. M.; Jansen, C. L.; Wertheim-van-Dillen, P. M. E.; van der Noordaa, J. *J. Clin. Microbiol.* **1990**, *28*, 495.
(6) Melzak, K. A.; Sherwood, C. S.; Turner, R. F. B.; Haynes, C. A. *J. Colloid Interface Sci.* **1996**, *181*, 635.
(7) Daniel, L. N.; Mao, Y.; Saffiotti, U. *Free Radicals Biol. Med.* **1993**, *14*, 463. Daniel, L. N.; Mao, Y.; Daniel, L. N.; Whittaker, N.; Saffiotti, U. *Environ. Health Perspect. Suppl.* **1994**, *102*, 165. Mao, Y.; Williams, A. O.; Saffiotti, U. *Scand. J. Work Environ. Health Suppl.* **1995**, *21*, 22.
(8) Heppleston, A. G. *Br. Med. Bull.* **1969**, *25*, 282.
(9) Carlisle, E. M. *Science* **1970**, *167*, 279.
(10) Hench, L. L. *J. Am. Ceram. Soc.* **1991**, *74*, 1487.
(11) Li, P.; Ye, X.; Kangasniemi, I.; de Blieck-Hogervorst, J. M. A.; Klein, C. P. A. T.; de Groot, K. *J. Biomed. Mater. Res.* **1995**, *29*, 325.
(12) Li, P.; Ohtsuki, C.; Kokubo, T.; Nakanish, K.; Soga, N.; Nakamura, T.; Yamamuro, T. *J. Am. Ceram. Soc.* **1992**, *75*, 2094.
(13) Leszczynski, J.; Kwiatkowski, J. S. *J. Phys. Chem.* **1993**, *97*, 1364. Kwiatkowski, J. S.; Leszczynski, J. *J. Phys. Chem.* **1992**, *96*, 6634. Kwiatkowski, J. S.; Leszczynski, J. *Mol. Phys.* **1992**, *76*, 475. Kwiatkowski, J. S.; Leszczynski, J. *J. Mol. Struct.* (*Theochem*) **1992**, *258*, 287.
(14) Sponer, J.; Hobza, P.; Leszczynski, J. In: *Computational Chemistry: Reviews of Current Trends*; Leszczynski, J., Ed. World Scientific Publication Co.: New York, 1996; Vol. I, pp 185−218. Sponer, J.; Leszczynski, J.; Hobza, P. *J. Phys. Chem. A* **1997**, *101*, 9489. Sponer, J.; Gabb, H. A.; Leszczynski, J.; Hobza, P. *J. Biophys.* **1997**, *73*, 76. Sponer, J.; Leszczynski, J.; Hobza, P. *J. Biomol. Struct. Dyn.* **1996**, *14*, 117. Sponer, J.; Leszczynski, J.; Vetterl, V.; Hobza, P. *J. Biomol. Struct. Dyn.* **1996**, *13*, 695. Sponer, J.; Leszczynski, J.; Hobza, P. *J. Phys. Chem.* **1996**, *100*, 5590. Sponer, J.; Florian, J.; Hobza, P.; Leszczynski, J. *J. Biomol. Struct. Dyn.* **1996**, *13*, 827. Florian, J.; Leszczynski, J. *J. Am. Chem. Soc.* **1996**, *118*, 3010.
(15) (a) *Gaussian 92/DFT*, Rev. F.2; Frisch, M. J.; Trucks, G. W.; Schlegel, H. B.; Gill, P. M. W.; Johnson, B. G.; Wong, M. W.; Foresman, J. B.; Robb, M. A.; Head-Gordon, M.; Replogle, E. S.; Gomperts, R.; Andres, J. L.; Raghavachari, K.; Binkley, J. S.; Gonzalez, C.; Martin, R. L.; Fox, D. J.; Defrees, D. J.; Baker, J.; Stewart, J. J. P.; Pople, J. A. Gaussian, Inc.: Pittsburgh, PA, 1992. *NBO*, Version 3.1; Glendening, E. D.; Reed, A. E.; Carpenter, J. E.; Weinhold, F. Gaussian, Inc.: Pittsburgh, PA, 1993. (b) Foresman, J. B.; Frisch, A. E. *Guide to Using Gaussian. Exploring Chemistry with Electronic Structure Methods*; Gaussian, Inc.: Pittsburgh, PA, 1993.
(16) Results of ab initio calculations at the HF/3-21G(d) and HF/3-21+G(d) levels can be obtained from the authors upon request.
(17) Hess, A. C.; McMillan, P. F.; O'Keeffe, M. *J. Phys. Chem.* **1987**, *91*, 1395.
(18) Sauer, J. *Chem. Phys. Lett.* **1983**, *97*, 275.
(19) Jayaram, B.; Mezei, M.; Beveridge, D. L. *J. Comput. Chem.* **1987**, *8*, 917.
(20) Liang, C.; Ewig, C. S.; Stouch, T. R.; Hagler, A. T. *J. Am. Chem. Soc.* **1993**, *115*, 1537.
(21) Becke, A. D. *J. Chem. Phys.* **1993**, *98*, 5648.
(22) Del Bene, J. E.; Person, W. B.; Szczepaniak, K. *J. Phys. Chem.* **1995**, *99*, 10705.
(23) Murashov, V. V.; Leszczynski, J. Manuscript in preparation.
(24) Saenger, W. *Principles of Nucleic Acid Structure*; Springer-Verlag: New York, 1984.
(25) Boys, S. F.; Bernardi, F. *Mol. Phys.* **1970**, *19*, 553.
(26) Mulliken, R. S. *J. Chem. Phys.* **1949**, *46*, 497.
(27) Hair, M. L.; Hertl, W. *J. Phys. Chem.* **1970**, *74*, 91.
(28) Schindler, P. W.; Stumm, W. In *Aquatic surface chemistry−chemical processes at the particle−water interface*; Wiley: New York, 1987; pp 83−110. Schindler, P. W.; Kamber, H. R. *Helv. Chim. Acta*. **1968**, *51*, 1781.
(29) *CRC Handbook of Chemistry and Physics*, 61st ed.; Weast, R. C., Ed.; CRC Press: Boca Raton, FL, 1980−1981.
(30) Stöber, W. *Adv. Chem. Ser.* **1967**, *67*, 161.
(31) Kubicki, J. D.; Apitz, S. E.; Blake, G. A. *Phys. Chem. Miner.* **1995**, *22*, 481.
(32) Newton, M. D.; Gibbs, G. V. *Phys. Chem. Miner.* **1980**, *6*, 221.
(33) Kubicki, J. D.; Blake, G. A.; Apitz, S. E. *Geochim. Cosmochim. Acta* **1997**, *61*, 1031.
(34) Pelmenschikov, A. G.; Morosi, G.; Gamba, A. *J. Phys. Chem. A* **1997**, *101*, 1178.
(35) Pullman, A.; Pullman, B.; Berthod, H. *Theor. Chim. Acta* **1978**, *47*, 175.
(36) Liebmann, P.; Loew, G.; McLean, A. D.; Pack, G. R. *J. Am. Chem. Soc.* **1982**, *104*, 691.
(37) Murashov, V. *Chem. Phys. Lett.* **1995**, *236*, 609.
(38) Landin, J.; Pascher, I.; Cremer, D. *J. Phys. Chem.* **1995**, *99*, 4471.
(39) Reed, A. E.; Schade, C.; Schleyer, P. v. R.; Kamath, P. V.; Chandrasekhar, J. *J. Chem. Soc., Chem. Commun.* **1988**, 67.
(40) Florian, J.; Baumruk, V.; Strajbl, M.; Bednarova, L.; Stepanek, J. *J. Phys. Chem.* **1996**, *100*, 1559.
(41) Corbridge, D. E. C. *The Structural Chemistry of Phosphates*; Elsevier: New York, 1974.
(42) Allen, F. H.; Kennard, O.; Watson, D. G.; Brammer, L.; Orpen, A. G.; Taylor, *J. Chem. Soc., Perkin Trans. 2* **1987**, S1−S19.
(43) Giarda, L.; Garbassi, F.; Calcaterra, M. *Acta Crystallogr.* **1973**, *B29*, 1826.
(44) Wiberg, K. B.; Hadad, C. M.; Lepage, T. J.; Breneman, C. M.; Frisch, M. J. *J. Phys. Chem.* **1992**, *96*, 671.
(45) Alexander, R. S.; Kanyo, Z. F.; Chirlian, L. E.; Christianson, D. W. *J. Am. Chem. Soc.* **1990**, *112*, 933.
(46) Nanda, R. K.; Govil, G. *Theor. Chim. Acta (Ber.)* **1975**, *38*, 71. Liebmann, P.; Loew, G.; McLean, A. D.; Pack, G. R. *J. Am. Chem. Soc.* **1982**, *104*, 691.
(47) Schneider, B.; Kabelac, M.; Hobza, P. *J. Am. Chem. Soc.* **1996**, *118*, 12207.
(48) Kyogoku, Y.; Iitaka, Y. *Acta Crystallogr.* **1966**, *21*, 49.
(49) West, J. *Z. Kristallogr.* **1930**, *74*, 306. Ubbelohde, A. R.; Woodward, I. *Proc. R. Soc., Ser. A* **1947**, *188*, 358. Bacon, G. E.; Pease, R. S. *Proc. R. Soc., Ser. A* **1955**, *230*, 359.
(50) Hadzi, D.; Hodoscek, M.; Grdadolnik, J.; Avbelj, F. *J. Mol. Struct.* **1992**, *266*, 9.
(51) Guan, Y.; Choy, G. S.-C.; Glaser, R.; Thomas, G. J., Jr. *J. Phys. Chem.* **1995**, *99*, 12054. Guan, Y.; Thomas, G. J., Jr. *J. Mol. Struct.* **1996**, *379*, 31.
(52) Scott, A. P.; Radom, L. *J. Phys. Chem.* **1996**, *100*, 16502.
(53) Shimanouchi, T.; Tsuboi, M.; Kyogoku, Y. *Adv. Chem. Phys.* **1964**, *7*, 435.
(54) Pelmenschikov, A. G.; Morosi, G.; Gamba, A. *J. Phys. Chem.* **1992**, *96*, 7422.
(55) Sinclair, P. E.; Catlow, C. R. A. *J. Chem. Soc., Faraday Trans.* **1997**, *93*, 333.
(56) Perahia, D.; Pullman, A.; Berthod, H. *Theor. Chim. Acta (Ber.)* **1975**, *40*, 47.
(57) Frischleder, H.; Gleichmann, S.; Krohl, A. *Chem. Phys. Lipids* **1977**, *19*, 144.
(58) Alagona, G.; Ghio, C.; Kollman, P. A. *J. Am. Chem. Soc.* **1983**, *105*, 5226.
(59) Schneider, B.; Patel, K.; Berman, H. M. *Prog. Biophys. Mol. Biol.* **1996**, *65*, PB105.
(60) Ichikawa, M. *Acta Crystallogr.* **1987**, *B43*, 23.
(61) Ferraris, G.; Ivaldi, G. *Acta Crystallogr.* **1984**, *B40*, 1.
(62) Souhassou, M.; Espinosa, E.; Lecomte, C.; Blessing, R. H. *Acta Crystallogr.* **1995**, *B51*, 661.
(63) Cruickshank, D. W. *J. Chem. Soc.* **1961**, 5485.
(64) Blessing, R. H. *Acta Crystallogr.* **1988**, *B44*, 334.
(65) Gelbin, A.; Schneider, B.; Clowney, L.; Hsieh, S.-H.; Olson, W. K.; Berman, H. M. *J. Am. Chem. Soc.* **1996**, *118*, 518.
(66) Gorenstein, D. O.; Findlay, J. B.; Momii, R. K.; Luxon, B. A.; Kar, D. *Biochemistry* **1976**, *5*, 3796.
(67) Sutherland, G. B. B. M.; Tsuboi, M. *Proc. R. Soc. London* **1957**, *A239*, 446.
(68) Prescott, B.; Steinmetz, W.; Thomas, G. J., Jr. *Biopolymers* **1984**, *23*, 235.
(69) Crowe, J. H.; Crowe, L. M.; Chapman, D. *Arch. Biochem. Biophys.* **1984**, *232*, 400.
(70) Arrondo, J. L. R.; Goni, F. M.; Macarulla, J. M. *Biochim. Biophys. Acta* **1984**, *794*, 165.
(71) Lerner, D. B.; Becktel, W. J.; Everett, R.; Goodman, M.; Kearns, D. R. *Biopolymers* **1984**, *23*, 2157.
(72) Okabayashi, H.; Yoshida, T.; Ikeda, T.; Matsuura, H.; Kitagawa, T. *J. Am. Chem. Soc.* **1982**, *104*, 5399.
(73) Pullman, A.; Pullman, B.; Berthod, H. *Theor. Chim. Acta* **1975**, *40*, 93.
(74) Frank, H. S.; Wen, W.-Y. *Discuss. Faraday Soc.* **1957**, *24*, 133. Del Bene, J.; Pople, J. A. *Chem. Phys. Lett.* **1969**, *4*, 426.
(75) Pudzianowski, A. T. *J. Phys. Chem.* **1996**, *100*, 4781.
(76) Sauer, J.; Ugliengo, P.; Garrone, E.; Saunders, V. R. *Chem. Rev.* **1994**, *94*, 2095.
(77) Krossner, M.; Sauer, J. *J. Phys. Chem.* **1996**, *100*, 6199.
(78) Kazansky, V. B.; Gitscov, A. M.; Andreev, V. M.; Zhidomirov, G. M. *J. Mol. Catal.* **1978**, *4*, 135.